Surface deformation caused by pressure changes in the fluid core

Ming Fang, Bradford H. Hager, Thomas A. Herring

Department of Earth, Atmospheric, and Planetary Sciences, Massachusetts Institute of Technology

Abstract. Pressure load Love numbers are presented for calculating the mantle deformation induced by the variation of the pressure field at the core mantle boundary (CMB). We find that the CMB geostrophic pressure fields, derived from "frozen-flux" core surface flow estimates at epochs 1965 and 1975, produce a relative radial velocity (RRV) field in the range of 3mm/decade with uplift near the equator and subsidence near the poles. The contribution of this mechanism to the change in the length of day (l.o.d) is small ---- about 2.3×10^{-2} ms/decade. The contribution to the time variation of the ellipticity coefficient J_2 is more important ---- about -1.3×10^{-11} /yr.

Introduction

It is generally believed, after Elsasser (1946), Roberts and Scott (1965), and Backus (1968), that the secular variation of the geomagnetic field (SV) is primarily due to the advection of pre-existing lines of magnetic force of the main field by the fluid motion just below the core mantle boundary (CMB). This "frozen-flux" mechanism enables us to probe the dynamic behavior of the fluid metallic core on the decadal time scale using observed SV. However, the inversion of the SV through the induction equation for the tangential flow near the CMB is highly underdetermined. One dynamical assumption that helps secure uniqueness is that the flow in the upper reaches of the core is in geostrophic balance with the pressure field there (Ball et al., 1969; Le Mouël et al., 1985, Backus and Le Mouël 1986).

Pressure variations at the CMB also cause deformation of the solid mantle. Thus, changes in the pattern of flow in the core result in deformation of Earth's surface. For world wide geodetic networks, this surface deformation is a potential source of signal that has not been explored before. If this surface deformation were large enough to be observed, and could be separated from other effects, it would provide an additional constraint on the dynamics of core flow. The transfer of net angular momentum from the core to the mantle via topographic coupling at the CMB (Hide, 1969; 1989) is an integrated global signal. In contrast, the surface deformation field is only a chart of local signals. Thus, pressure variations associated with geostrophic flow, and perhaps higher order flows, as well, can not escape influencing the deformation field. In this paper we use the geostrophic pressure variations derived from core flow models (Gire et al., 1990) to calculate the radial deformation of Earth's surface. This deformation in turn affects Earth rotation by changing the moment of inertia. We also examine this two-way interaction by calculating the change in the l.o.d and the time variation of the ellipticity coefficient J_2 induced by the deformation field.

Pressure load Love number

The only difference between a mass load and a pressure load is that a pressure load has no load mass contribution to the perturbation of the gravity potential. The pressure field external to the solid earth acts upon the earth as a surface load, thus, the so called "pressure load Love numbers" for the external field can be easily defined and calculated by slightly modifying Longman's

(1962) classical mass load theory (see below). The pressure perturbation in the interior of the earth, on the other hand, is a three dimensional scalar field like a mass perturbation field. The Green functions for responses to the internal pressure perturbation should be similar to the Green functions for the responses to the internal mass density perturbation (e.g., Richards and Hager, 1984). Practically, it is difficult to estimate the pressure perturbation as a function of depth using the SV data, but we can estimate the pressure variation near the CMB (see below). In this situation, we treat the mantle as a spherical shell which is subjected to a pressure load at the CMB, assuming that the pressure perturbation within the mantle is only induced by the pressure load at the CMB. This problem is similar to the external pressure load problem. The scope of this paper is limited to such a "pressure load" problem, so, we use the nomenclature "pressure load Love number at the CMB". The nomenclature "internal pressure Love number" used by Lefftz and Legros (1992) is more proper for describing the three dimensional pressure perturbation problem.

We define pressure load Love numbers at harmonic degree n, $h_n(r)$, $l_n(r)$, and $k_n(r)$, as

$$U_n(r) = \frac{3q(r_0)}{4\pi r_0^2 \, g\bar{\rho}} h_n(r), \quad V_n(r) = \frac{3q(r_0)}{4\pi r_0^2 \, g\bar{\rho}} l_n(r)$$
$$\Phi_n(r) = \frac{3q(r_0)}{4\pi r_0^2 \, \bar{\rho}} k_n(r) \tag{1}$$

where $U_n(r)$, $V_n(r)$, and $\Phi_n(r)$ are the radial, horizontal, and gravity perturbation components, respectively (see Longman, 1962 for details), q is a point force load located at position $(r_0,0,0)$, g is the outer surface gravity, and $\bar{\rho}$ is the average density of the earth (note, the point force load q has the dimension of a body force). The radial deformation, s_r, and the gravity potential disturbance, ϕ_r, at radius r are

$$\begin{bmatrix} s_r \\ \phi_r \end{bmatrix}(\theta,\varphi) = \int_\sigma \mathrm{K}_{\begin{bmatrix} h \\ k \end{bmatrix}}(r,\alpha)\, p(\theta',\varphi')\, d\sigma'$$
$$\mathrm{K}_{\begin{bmatrix} h \\ k \end{bmatrix}}(r,\alpha) = \frac{3}{4\pi g\bar{\rho}} \sum_n \begin{bmatrix} h_n(r) \\ k_n(r)\,g \end{bmatrix} \mathrm{P}_n(\cos\alpha) \tag{2}$$

where p is the pressure field, α is the arc length between the fixed point (ϑ,φ) and the moving point (ϑ',φ'), and P_n is the Legendre polynomial. The integral in (2) is over the pressure distribution on a unit sphere.

We see from (1) that the response at r also depends upon the radius r_0 where the point load is applied. For the point force load q acting on the outer surface of the earth, $r = a$, these pressure load Love numbers for the surface response, $r_0 = a$, are compatible with the mass load Love numbers (Longman, 1962). The fluid core comes into effect through the free slip boundary conditions at the CMB (e.g., Richards and Hager, 1984).

Fig. 1 displays different pressure load Love numbers based on the seismic earth model PREM (Dziewonski and Anderson, 1981). In the cases of CMB pressure load, a comparison between the CMB response **pcc** and the surface response **pcs** shows that

the mantle acts as a low-pass filter for the surface response pcs, with the cut-off frequency at about degree 9. As is well known, the "frozen flux" approximation only works on a fairly large spatial scale (>600 km) (e.g., Roberts and Scott, 1965). The implied upper limit in harmonic degree of about 36 is much higher than degree 9. Hence, as far as the surface deformation is concerned, the "frozen flux" approximation should be accurate.

Geostrophic pressure field at the CMB

For a tangentially geostrophic flow, the horizontal velocity **u** and the pressure p at the CMB are related through the horizontal momentum equation (e.g., Le Mouël et al., 1985)

$$2\rho b\,\Omega\cos\vartheta\,\mathbf{u} = \hat{\mathbf{n}} \times \nabla_H\, p \qquad (3)$$

where ρ is the density of the core, Ω is the angular velocity of the earth's rotation, $\hat{\mathbf{n}}$ the radial unit vector, and ∇_H the horizontal gradient operator on a unit sphere. Once the flow field **u** is known, we can infer p from **u** by using equation (3) (e.g., Gire et al, 1990). Because of the gradient operator ∇_H , a pressure field so obtained misses the zero degree term corresponding to a uniform dilation or compression along the radius. This is of little interest in analyzing the spatial variation of the deformation field. For simplicity, we assume that the zero degree terms in the pressure field at different epochs are all the same, and thus, set the reference for the pressure field such that the degree zero terms are zero.

A number of geostrophic, steady flow models, **u**, have been produced by selectively inverting the SV data collected over the period 1840-1990 (e.g., Gire et al, 1986; Voorhies, 1988, 1991; Bloxham, 1989; Gire et al., 1990; Jackson et al., 1993). As noted by Hide et al. (1993), most of these steady flow models are similar in appearance. Recently, a time-varying flow model has been proposed (Voorhies, 1995). A time-varying flow model enables calculation of dynamical surface deformation. A simple dimensional analysis shows that the contribution of the inertial term in the elastodynamic equation is negligible, so, it is sufficient to estimate the surface velocity by using the quasi-static deformation at successive epochs. In this study, we use the primitive, relatively rough steady flow models G6070.3 and G8070.3 (Voorhies, 1988). These models were derived by fitting the Definitive Geomagnetic Reference Field (DGRF) model from 1960-1970 and from 1980-1970 respectively. We set the average epochs for the two time intervals to 1965 and 1975 respectively. Because of the strong low-pass filter effect, a change in smoothness of the model flow does not have much impact on the surface deformation. Fig. 2 shows the CMB pressure fields computed from G6070.3 and G8070.3.

Results

Fig. 3 and 4 are the radial deformation fields calculated using equation (3). The summation of harmonic degrees starts from degree 2; thus, the deformation fields only represent the departure from the initial state, presumed to be hydrostatic equilibrium, and do not depend upon the choice of the origin of the coordinate. Comparing Fig. 2 and Fig. 3, we can see that the small scale features in the pressure fields have been filtered out in the surface deformation fields, although the pressure fields themselves are

not very detailed (only up to degree 16). The horizontal deformation is, in general, much smaller than the radial deformation, and will not be discussed in this paper.

The relative radial velocity (RRV) fields in Fig. 4 are obtained by subtracting the radial deformation at the "1965" epoch from its counterpart at the "1975" epoch. A striking feature of the RRV fields, both at the CMB and the surface, is that the relative radial motion between the "1965" epoch and the "1975" epoch is roughly centered around a pole (RRV pole) near (60° N, 120° E). This "1975" RRV pole is roughly on the opposite side, with respect to the North pole, from the 1975 geomagnetic pole at (78.6° N, 70.5° W) (e.g., Rikitake and Honkura, 1985). There is compression near the RRV poles and dilation near the equator relative to the RRV poles. This structure seems to suggest a strong influence of the earth's rotation on the RRV field. If, instead of the Coriolis force, we put the centrifugal force in (3), we would expect a deformation field similar to Fig. 4 but centered at the rotation axis.

The flattening of the figure along the RRV poles increases the moment of inertia about the rotation axis and slows down Earth rotation. This deformation mechanism differs from that of topographic coupling (Hide, 1969, 1989). We calculate the change in the l.o.d caused by this two-way interaction mechanism using the relation

$$\delta(\text{l.o.d}) = (\text{l.o.d})\frac{\delta c_{33}}{C_m} \tag{4}$$

where C_m is the mean polar moment of inertia of the mantle, and δc_{33} is the difference in perturbation of the mantle polar moment of inertia, c_{33}, between different epochs. Using equation (2), we have

$$\delta c_{33} = \frac{8\pi\delta w_{20}}{\sqrt{125\, g\bar{\rho}}} \int_b^a \left(\frac{d\rho}{dr} h_2 + \rho \frac{dh_2}{dr} \right) r^4 dr \tag{5}$$

where w_{20} is the degree 2 zonal harmonic coefficient of the CMB pressure field (fully normalized). For the PREM earth model, G6070.3 and G8070.3 flow models, and the value $C_m = 7.2 \times 10^{37}\ \text{kg m}^2$, we obtain

$$\delta(\text{l.o.d}) = 2.3 \times 10^{-2}\ \text{ms / decade} \tag{6}$$

From (5), we can also calculate the time variation of the ellipticity coefficient J_2 using the conservation of the trace of the inertia tensor (Rochester and Smylie, 1974):

$$\dot{J}_2 = -1.3 \times 10^{-11}\ /\ \text{yr} \tag{7}$$

Discussion

The predicted δ(l.o.d) in (6) is two to four orders of magnitude smaller than predicted based on the CMB topographic coupling mechanism (e. g. Jackson et al, 1993; Hide et al, 1993). It is also below the noise level of the observed decadal fluctuation in l.o.d (e.g., Lambeck, 1980). On the other hand, the predicted $\dot{J}_2$ in (7) is quite large. Although the complete separation of $\dot{J}_2$ from the lumped contribution of all even zonal harmonics is still at issue, there is no question that $\dot{J}_2$ dominates

the observed satellite nodal drift. If we take the observed $\dot{J}_2$ as about -2.5×10^{-11}/yr (Cheng et al, 1989), our prediction would provide about 50% of the observed $\dot{J}_2$. This mechanism has been overlooked in previous investigations. There are other mechanisms, such as postglacial rebound (Peltier, 1985), and present-day Antarctic mass changes (James and Ivins, 1995), which could predict comparably important $\dot{J}_2$. The uncertainty in the present-day secular ice mass changes in Antarctica results in predictions of $\dot{J}_2$ ranging from -4.1×10^{-11}/yr to 1.8×10^{-11}/yr (James and Ivins, 1995). Lefftz and Legros (1992) found that if the zonal harmonic component of the CMB topography has an amplitude of 15 m and lasts for 5000 years, the viscoelastic relaxation of the earth would contribute to $\dot{J}_2$ by about -2.4×10^{-11} / yr. These previous results, plus our calculations, indicate that the observed $\dot{J}_2$ is a lumped signal that should not be attributed to a single causal mechanism.

The amplitude of the surface RRV field (Fig. 4) is in the range of 3mm/decade. Although a signal of this magnitude is in principle observable with a global VLBI network (e.g., Herring 1995), it is substantially smaller than other geodynamic signals, such as post glacial rebound. In fact, 3 mm/10yr is even smaller than the uncertainties in the estimated deformations induced by post glacial rebound (e.g., Mitrovica et al., 1994). Thus, at the current sensitivity, it is more likely to be lost in the noise of other geophysical processes. But we have to bear in mind that the theoretical framework for the dynamo is still incomplete. If pressure changes associated with the ageostrophic component of the flow are large, the associated RRV would also increase. But we can be certain from this investigation that no matter how the theory develops in the future, no detailed information beyond harmonic degree 9 about the CMB pressure variation will be contained in potentially observable surface deformation. Finally, our analysis of the RRV is based on the steady geostrophic flow models at the average epochs "1965" and "1975". There is no obvious evidence to assert that the RRV in Fig. 4 will remain for a longer period of time. If Fig. 4 is only a snapshot of a rapidly changing movie, it will be even more difficult to measure the RRV using geodetic means.

Acknowledgments. We thank Drs. R. Hide, C. V. Voorhies, D. Dong, and W. Kuang for discussions. This study was supported by NASA DOSE grant NAG5-1911.

References

Backus, G., Kinematics of geomagnetic secular variation in a perfectly conducting core, *Phil. Trans. Roy. Soc., Lond.* **A263**, 239-266, 1968.

Backus, G. and J.-L. LeMouël, The region on the core-mantle boundary where a geostrophic velocity field can be determined from frozen-flux geomagnetic data, *Geophys. J. R. Astron. Soc.*, **85,** 617-628, 1986.

Ball, R. H., A. B. Kahle, and E. H. Vestine, Determination of surface motions of the earth's core, *J. Geophys. Res.*, **74,** 3659-4680, 1969.

Bloxham, J., Simple models of fluid flow at the core surface derived from geomagnetic field models, *Geophys. J. Int.*, **99,** 173-182, 1989.

Cheng, M. K., R. J. Eanes, C. K. Shum, B. E. Schutz, and B. D. Tapley, Temporal variations in low degree zonal harmonics

from Starlette orbit analysis, *Geophys. Res. Lett.*, **16**, 393-396, 1989.

Dziewonski, A. M. and D. Anderson, Preliminary reference Earth model, *Phys. Earth Planet. Inter.* 25, 297-356, 1981.

Elsasser, W. M., Induction effects in terrestrial magnetism: I theory, *Phys. Rev.*, **69**, 106-116, 1946.

Gire, C., J.-L. LeMouël, and T. Madden, Motions at the core surface derived from SV data, *Geophys. J. R. Astron. Soc.* **84**, 1-29, 1986.

Gire, C., J.-L. LeMouël, Tangentially geostrophic flow at the core-mantle boundary compatible with the observed geomagnetic secular variation: the large-scale component of the flow, *Phys. Earth Planet. Inter.* **59**, 259-287, 1990.

Herring, T. A., VLBI data, acquisition, environmental effects, *Rev. Geophys.*, **33**, 345, 348, 1995.

Hide, R., Interaction between the earth's liquid core and solid mantle, *Nature*, **222**, 1055-1056, 1969.

Hide, R., Fluctuation in the earth's rotation and the topography of the core-mantle interface, *Phil. Trans. Roy. Soc. Lond.* **A328**, 351-363, 1989.

Hide, R., R. W. Clayton, B. H. Hager, M. A. Speith, and C. V. Voorhies, Topographic core-mantle coupling and fluctuations in the earth's rotation, in *Relating Geophysical Structures and Processes,* Geophys. Monogr. Ser., Vol. **76,** ed. K. Aki and R. Dmowska, pp. 107-120, AGU, Washington D. C., 1993.

Jackson, A., J. Bloxham, and D. Gubbins, Time-dependent flow at the core surface and conservation of angular momentum in the coupled core-mantle system, in *Dynamics of Earth's Deep Interior and Earth Rotation*, Geophys. Monogr. Ser., Vol. **72,** ed. J.-L. LeMouël, D. E. Smylie, and T. A. Herring, pp 97-107, AGU, Washington D. C., 1993.

James, T. S. and E. R. Ivins, Present-day Antarctic ice mass changes and crustal motion, *Geophys. Res. Lett.*, **22**, No. **8,** 973-976, 1995.

Lambeck K. *The Earth's Variable Rotation*, Cambridge Uni. Press, 1980.

Lefftz, M., and H. Legros, Influence of viscoelastic coupling on the axial rotation of the earth and its fluid core, *Geophy. J. Int.* **108,** 725-739, 1992.

LeMouël, J.-L., C. Gire, and T. Madden, Motions at the core surface in the geostrophic approximation, *Phys. Earth Planet. Inter.* **39**, 270-287, 1985.

Longman, I. M., A Green function for determining the deformation of the earth under surface mass load, 1, Theory, *J. Geophys. Res.*, **67,** 845-850, 1962.

Mitrovica, J., J. L. Davis, and I. I. Shapiro, A spectral formulism for computing three-dimensional deformations due to surface loads 2. Present day glacial isostatic adjustment, *J. Geophys. Res.*, **99**, 7075-7101, 1994.

Peltier, W. R., The LAGEOS constraint on deep mantle viscosity, *J. Geophys. Res.*, **91**, 9411-9421, 1985.

Richards, M. and B. H. Hager, Geoid anomalies in a dynamic Earth, *J. Geophys. Res.*, **89**, 5987-6002.

Rochester, M. G., and D. E. Smylie, On the changes in the earth's inertia tensor, *J. Geophys. Res.*, **79**, 4948-4951.

Rikitake, T. and Honkura, Y., *Solid Earth Geomagnetism*, Terra Sci. Pub. Tokyo. 1985.

Roberts, P. H. and S. Scott, On analysis of secular variation, 1, A hydromagnetic constraint, *J. Geomagn. Geoelectr.*, **17**, 137-151, 1965.

Voorhies, C. V., Probing surface core motions with DGRF models (abstract), *EOS Trans. AGU*, **69**, 336, 1988.

Voorhies, C. V., Coupling an inviscid core to an electrically-insulating mantle, *J. Geomag. Geoelect.*, **43**, 131-156, 1991.

Voorhies, C. V., Time-varying fluid flow at the top of Earth's core derived from definitive geomagnetic reference field models, *J. Geophys. Res.*, **100**, 10,029-10,039, 1995.

M. Fang, B. H. Hager, and T. A. Herring 54-614, MIT, Cambridge, MA. 02139

(Received: October 17, 1995
Accepted: January 25, 1996.)

Fig. 1. The spectra of radial and gravity load Love numbers h_n and k_n. The spectrum of each type is indicated by a thin line. The code **p** means pressure load, **m** means mass load, **s** denotes the earth's surface, **c** denotes the core mantle boundary (CMB). Thus, **pcs** represents the pressure load at the CMB and surface response, and so on. The minus sign indicates the direction of the load at the surface.

Fig. 2. The CMB geostrophic pressure fields at the average epochs 1965 and 1975. The tangential velocity models used for the conversion (equation (3) in the text) are from Voorhies (1988). Note, there are no degree zero components in these pressure fields.

Fig. 3. The radial surface deformations at the average epochs 1965 and 1975.

Fig. 4. The relative radial velocity (RRV) at the surface and the CMB respectively, obtained by subtracting the 1965 radial deformation from the 1975 radial deformation (see Fig. 3). The white dot marks the location of the geomagnetic pole at the epoch 1975 (e. g., Rikitake and Honkura, 1985). It roughly shares the same great circle with the RRV pole flanking the geographic North pole.

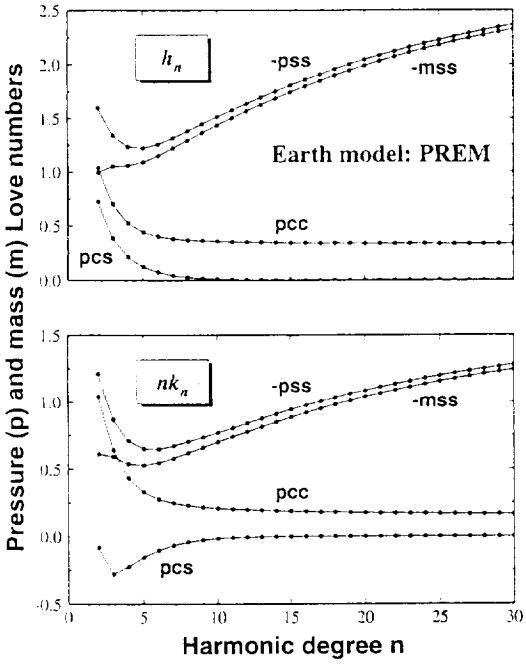
h_n
-pss
-mss
Earth model: PREM
pcc
pcs
nk_n
-pss
-mss
pcc
pcs
Pressure (p) and mass (m) Love numbers
Harmonic degree n

Fig 1.

"1965" Geostrophic pressure at CMB

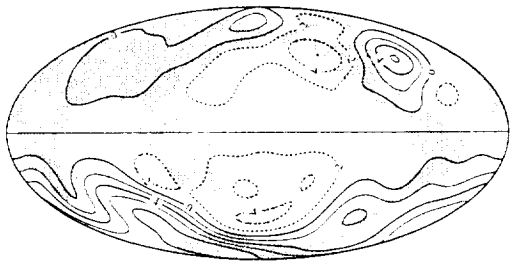

"1975" Geostrophic pressure at CMB

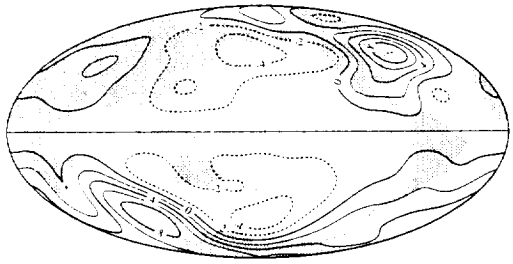

Fig 2

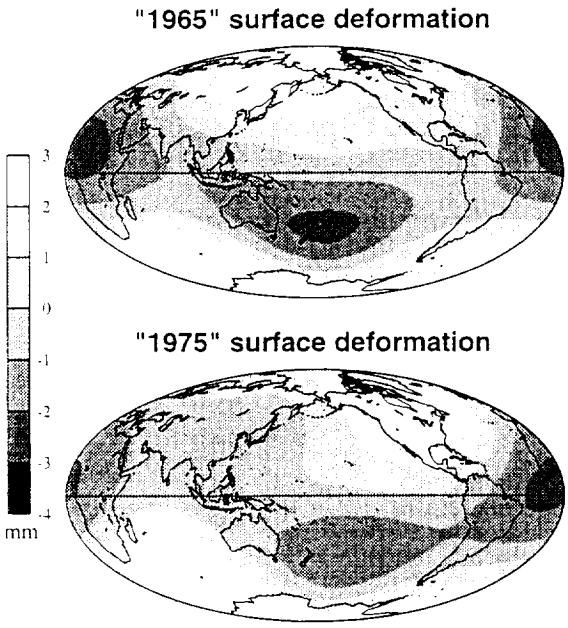
"1965" surface deformation
"1975" surface deformation
3
2
1
0
-1
-2
-3
-4
mm

F.93.

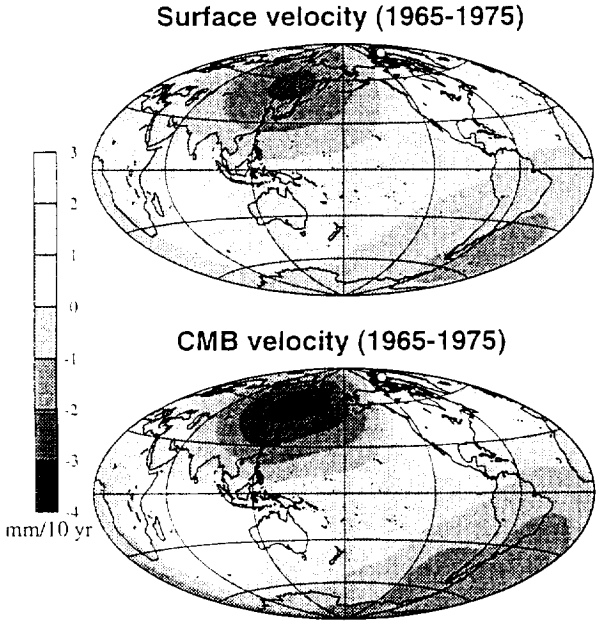
Surface velocity (1965-1975)
3
2
1
0
-1
-2
-3
-4
mm/10 yr
CMB velocity (1965-1975)

F.9.4